Available online at www.sciencedirect.com
SCIENCE DIRECT®
International Journal of Heat and Fluid Flow 26 (2005) 622–634
International Journal of HEAT AND FLUID FLOW
www.elsevier.com/locate/ijhff

Numerical computation of magnetothermal convection of water in a vertical cylindrical enclosure

Masato Akamatsu [a,*], Mitsuo Higano [a], Yoshio Takahashi [a], Hiroyuki Ozoe [b]

[a] Faculty of Systems Science and Technology, Akita Prefectural University, 84-4 Tsuchiya-Ebinokuchi, Honjo, Akita 015-0055, Japan
[b] Institute for Materials Chemistry and Engineering, Kyushu University, Kasuga Koen 6-1, Kasuga 816-8580, Japan

Accepted 29 March 2005
Available online 1 June 2005

Abstract

Numerical computations were carried out to clarify the effect of Kelvin force on the flow of water in a vertical cylindrical enclosure heated from below and cooled from above under a vertical magnetic field gradient. Since the Kelvin force that is produced by the magnetic field gradient depends on the position and the size of a circular electric coil, the coil was placed at either the hot or the cold plate and the coil diameter was set to be 2.5 or 5 times that of the enclosure. First, to understand the mechanism of the generation of the magnetothermal convection induced by the Kelvin force alone, the transition of velocity and temperature fields were visualized under a non-gravitational field. Under a gravitational field, the average Nusselt number decreased with increase of magnetic strength when the coil was placed at the lower end plate which was heated isothermally so that the generation of natural convection was suppressed by the Kelvin force. On the contrary, the average Nusselt number increased with increase of magnetic strength when the coil was placed at the upper end plate which was cooled isothermally so that the natural convection was enhanced by the Kelvin force.

Keywords: Kelvin force; Magnetothermal convection; Natural convection; Water; Diamagnetic fluid; Vertical cylindrical enclosure

1. Introduction

Many reports on the interaction between a magnetic field and a fluid have appeared. For example, the control of thermal convection in a liquid metal with high electric conductivity (Chandrasekhar, 1981) and the control of ferromagnetic fluid without electric conductivity (Rosensweig, 1985) have been extensively studied from the basics to the application. The purpose of the present study is to control the convection of a diamagnetic fluid without electric conductivity by a magnetic field. In an electrically conducting fluid such as mercury, the force acting on the fluid is the Lorentz force. On the other hand, in an electrically non-conducting fluid such as air or water, the force acting on the fluid is the Kelvin force (Gray et al., 2001). This force is called a magnetic or magnetizing force in the field of engineering. The Kelvin force is produced only under inhomogeneous magnetic field. The Lorentz force, however, is produced under both homogeneous and inhomogeneous magnetic fields.

Regarding Kelvin force, Faraday (1847) examined the effect of magnetic field on flame and gases using an electromagnet. Pauling et al. (1946) developed an instrument for determining the partial pressure of oxygen in a gas by using Kelvin force. Carruthers and Wolfe (1968) reported the effect of magnetic field on oxygen gas in a rectangular container with a thermal gradient by using an electromagnet. Then, in the 1990s, by the development of a super-conducting magnet that does not require liquid helium, investigations to determine the

* Corresponding author. Tel.: +81 184 27 2118; fax: +81 184 27 2188.
E-mail address: akamatsu@akita-pu.ac.jp (M. Akamatsu).

0142-727X/$ - see front matter © 2005 Elsevier Inc. All rights reserved.
doi:10.1016/j.ijheatfluidflow.2005.03.008

Nomenclature

$\vec{b}$	magnetic induction [T]
$\vec{B}$	$= \vec{b}/b_0$, dimensionless magnetic induction [–]
c_p	specific heat capacity at constant pressure [J/(kg K)]
$\vec{f}_m$	Kelvin force [N/m^3]
g	gravitational acceleration [m/s^2]
h	$= r_0$, radius of a vertical cylindrical enclosure [m]
HR	$= h/r_0 = 1$, dimensionless radius of a vertical cylindrical enclosure [–]
HZ	$= 2$HR, dimensionless height of a vertical cylindrical enclosure [–]
i	electric current in a circular electric coil [A]
Nu_{ave}	$= \frac{\int_0^{2\pi}\int_0^{HR}\left(\frac{\partial T_{conv}}{\partial Z}\right)_{Z=0,HZ} R\cdot dR\cdot d\varphi}{\int_0^{2\pi}\int_0^{HR}\left(\frac{\partial T_{cond}}{\partial Z}\right)_{Z=0,HZ} R\cdot dR\cdot d\varphi}$, average Nusselt number at the end plate [–]
p	pressure [Pa]
p'	perturbed pressure [Pa]
P	$= p'/p_0$, dimensionless pressure [–]
Pr	$= \nu/\alpha$, Prandtl number [–]
r	radial coordinate [m]
R	$= r/r_0$, dimensionless radial coordinate [–]
Ra	$= g\beta(\theta_h - \theta_c)r_0^3/(\alpha\nu)$, Rayleigh number [–]
$d\vec{s}$	electric coil element [m]
$d\vec{S}$	$= d\vec{s}/r_0$ [–]
t	time [s]
T	$= (\theta - \theta_0)/(\theta_h - \theta_c)$, dimensionless temperature [–]
u	velocity in the radial direction [m/s]
U	$= u/u_0$, dimensionless velocity in the radial direction [–]
v	velocity in the circumferential direction [m/s]
V	$= v/u_0$, dimensionless velocity in the circumferential direction [–]
w	velocity in the axial direction [m/s]
W	$= w/u_0$, dimensionless velocity in the axial direction [–]
z	axial coordinate [m]
Z	$= z/r_0$, dimensionless axial coordinate [–]
Z_{co}	distance from the hot plate to the circular electric coil [–]

Greeks

α	thermal diffusivity [m^2/s]
β	volumetric coefficient of expansion [1/K]
γ	$= \chi_{m0}b_0^2/(\xi g r_0)$, ratio of Kelvin force to gravitational force [–]
θ	temperature [K]
θ_0	$= (\theta_h + \theta_c)/2$, reference temperature [K]
θ_c	cold plate temperature [K]
θ_h	hot plate temperature [K]
λ	thermal conductivity [W/(m K)]
μ	viscosity [Pa s]
ν	kinematic viscosity [m^2/s]
ξ	magnetic permeability in a vacuum [H/m]
ρ	density [kg/m^3]
ρ_0	density at the reference temperature [kg/m^3]
τ	$= t/t_0$, dimensionless time [–]
χ_m	mass magnetic susceptibility [m^3/kg]
χ_{m0}	$= \chi_m$, mass magnetic susceptibility at the reference temperature [m^3/kg]
χ_v	$= \rho\chi_m$, volumetric magnetic susceptibility [–]
φ	circumferential coordinate [rad]

Subscripts

ave	average
c	cold plate
co	circular electric coil
cond	conductive heat transfer
conv	convective heat transfer
h	hot plate
max	maximum
Z	axial component
0	reference value for dimensionless variable

effect of a strong magnetic field were rigorously carried out in various fields such as chemistry, biology, and engineering, and many interesting phenomena, such as that by Wakayama (1991a,b), Berry and Geim (1997), Uetake et al. (1999), Tagami et al. (1999), etc., have been reported. Reports on the Kelvin force related to the present study include those by Braithwaite et al. (1991), Wakayama's group (Bai et al., 1999; Qi et al., 1999, 2001a,b; Wakayama et al., 1997), Gray et al. (2001), and Ozoe's group (Akamatsu et al., 2003, 2005; Kaneda et al., 2002a,b,c; Maki et al., 2002; Shigemitsu et al., 2003; Tagawa et al., 2001, 2002a,b, 2003), in which the control of convection in paramagnetic and diamagnetic fluids in enclosures were investigated.

The present study focuses on how a Kelvin force affects the flow of water with the diamagnetic property in an enclosure with a thermal gradient. Therefore, numerical computations were carried out to clarify the effect of Kelvin force on the flow of water in a vertical cylindrical enclosure heated from below and cooled from above under a vertical magnetic field gradient.

2. Governing equations

The Kelvin force acting on a fluid is given as follows, according to Carruthers and Wolfe (1968):

$$\vec{f}_{\mathrm{m}} = \frac{\chi_{\mathrm{v}}}{2\xi}\vec{\nabla}b^2 = \frac{\rho\chi_{\mathrm{m}}}{2\xi}\vec{\nabla}b^2, \tag{1}$$

where $\chi_{\mathrm{v}} = \rho\chi_{\mathrm{m}}$ is the volumetric magnetic susceptibility, ρ is the density, χ_{m} is the mass magnetic susceptibility and ξ is the magnetic permeability in a vacuum.

The Kelvin force is a body force. Under an inhomogeneous magnetic field, this force is generated and can be included in the Navier–Stokes equation:

$$\rho\frac{\mathrm{D}\vec{u}}{\mathrm{D}t} = -\vec{\nabla}p + \mu\nabla^2\vec{u} + \frac{\rho\chi_{\mathrm{m}}}{2\xi}\vec{\nabla}b^2 + \rho\vec{g}, \tag{2}$$

where μ is the viscosity.

At the reference state of the isothermal state, there will be no convection. Therefore, Eq. (2) becomes:

$$0 = -\vec{\nabla}p_0 + \frac{\rho_0\chi_{\mathrm{m0}}}{2\xi}\vec{\nabla}b^2 + \rho_0\vec{g}, \tag{3}$$

where ρ_0 and χ_{m0} are, respectively, the density and the mass magnetic susceptibility at the reference temperature.

Pressure p can be represented by the summation of p_0 at the isothermal state of the reference temperature and p' at the perturbed state:

$$p = p_0 + p'. \tag{4}$$

In the non-isothermal state, convection will occur due to the differences of density and the mass magnetic susceptibility. Cini and Torrini (1968) reported that the magnetic susceptibility of water was dependent on temperature. However, in the temperature range from 0 to 80 °C, the change of magnetic susceptibility is minute. Therefore, it was considered that the mass magnetic susceptibility of water was independent of temperature in the present numerical computations. Therefore, subtracting Eq. (3) from Eq. (2) gives:

$$\rho\frac{\mathrm{D}\vec{u}}{\mathrm{D}t} = -\vec{\nabla}p' + \mu\nabla^2\vec{u} + \frac{(\rho-\rho_0)\chi_{\mathrm{m0}}}{2\xi}\vec{\nabla}b^2 + (\rho-\rho_0)\vec{g}. \tag{5}$$

By a Taylor expansion around a static state:

$$\rho = \rho_0 + (\partial\rho/\partial\theta)_0(\theta-\theta_0) + \cdots, \tag{6}$$

where

$$\beta = -\{(\partial\rho/\partial\theta)/\rho\}_0. \tag{7}$$

β is the volumetric coefficient of expansion. With the Boussinesq approximation, physical properties are constant at $\theta = \theta_0$.

Eq. (5) becomes:

$$\frac{\mathrm{D}\vec{u}}{\mathrm{D}t} = -\frac{\vec{\nabla}p'}{\rho_0} + \nu\nabla^2\vec{u} - \frac{\chi_{\mathrm{m0}}}{2\xi}\beta(\theta-\theta_0)\vec{\nabla}b^2 - \beta(\theta-\theta_0)\begin{pmatrix}0\\0\\-g\end{pmatrix}, \tag{8}$$

where ν is the kinematic viscosity.

The dimensionless governing equations in cylindrical coordinates become as follows. The equation of continuity becomes:

$$\frac{1}{R}\frac{\partial}{\partial R}(RU) + \frac{1}{R}\frac{\partial V}{\partial\varphi} + \frac{\partial W}{\partial Z} = 0. \tag{9}$$

The momentum equation in the radial direction becomes:

$$\begin{aligned}&\frac{\partial U}{\partial\tau} + U\frac{\partial U}{\partial R} + \frac{V}{R}\frac{\partial U}{\partial\varphi} + W\frac{\partial U}{\partial Z} - \frac{V^2}{R}\\ &\quad= -\frac{\partial P}{\partial R} + Pr\left[\frac{\partial}{\partial R}\left\{\frac{1}{R}\frac{\partial}{\partial R}(RU)\right\}\right.\\ &\qquad\left.+\frac{1}{R^2}\frac{\partial^2 U}{\partial\varphi^2} + \frac{\partial^2 U}{\partial Z^2} - \frac{2}{R^2}\frac{\partial V}{\partial\varphi}\right] - \frac{1}{2}\gamma RaPrT\frac{\partial B^2}{\partial R}.\end{aligned} \tag{10}$$

The momentum equation in the circumferential direction becomes:

$$\begin{aligned}&\frac{\partial V}{\partial\tau} + U\frac{\partial V}{\partial R} + \frac{V}{R}\frac{\partial V}{\partial\varphi} + W\frac{\partial V}{\partial Z} + \frac{UV}{R}\\ &\quad= -\frac{1}{R}\frac{\partial P}{\partial\varphi} + Pr\left[\frac{\partial}{\partial R}\left\{\frac{1}{R}\frac{\partial}{\partial R}(RV)\right\}\right.\\ &\qquad\left.+\frac{1}{R^2}\frac{\partial^2 V}{\partial\varphi^2} + \frac{\partial^2 V}{\partial Z^2} + \frac{2}{R^2}\frac{\partial U}{\partial\varphi}\right] - \frac{1}{2}\gamma RaPrT\frac{\partial B^2}{\partial\varphi}.\end{aligned} \tag{11}$$

The momentum equation in the axial direction becomes:

$$\begin{aligned}&\frac{\partial W}{\partial\tau} + U\frac{\partial W}{\partial R} + \frac{V}{R}\frac{\partial W}{\partial\varphi} + W\frac{\partial W}{\partial Z}\\ &\quad= -\frac{\partial P}{\partial Z} + Pr\left[\frac{1}{R}\frac{\partial}{\partial R}\left(R\frac{\partial W}{\partial R}\right) + \frac{1}{R^2}\frac{\partial^2 W}{\partial\varphi^2} + \frac{\partial^2 W}{\partial Z^2}\right]\\ &\qquad- \frac{1}{2}\gamma RaPrT\frac{\partial B^2}{\partial Z} + RaPrT.\end{aligned} \tag{12}$$

The energy equation becomes:

$$\begin{aligned}&\frac{\partial T}{\partial\tau} + U\frac{\partial T}{\partial R} + \frac{V}{R}\frac{\partial T}{\partial\varphi} + W\frac{\partial T}{\partial Z}\\ &\quad= \frac{1}{R}\frac{\partial}{\partial R}\left(R\frac{\partial T}{\partial R}\right) + \frac{1}{R^2}\frac{\partial^2 T}{\partial\varphi^2} + \frac{\partial^2 T}{\partial Z^2}.\end{aligned} \tag{13}$$

The distribution of magnetic induction was computed by Biot–Savart's law as seen in Eq. (14), as

$$\vec{B} = -\frac{1}{4\pi}\oint\frac{\vec{R}\times\mathrm{d}\vec{S}}{R^3}. \tag{14}$$

In the present numerical computations, we considered the axial symmetry system in a vertical cylindrical enclosure as the first step of research to clarify the mechanism of the magnetothermal convection of water under the Kelvin force. Hence, in Eqs. (9)–(13), all the derivatives in a circumferential direction become zero. The following dimensionless variables were employed in the above equations:

$$R=\frac{r}{r_0},\quad Z=\frac{z}{r_0},\quad \tau=\frac{t}{t_0},$$
$$U=\frac{u}{u_0},\quad V=\frac{v}{u_0},\quad W=\frac{w}{u_0},$$
$$P=\frac{p'}{p_0},\quad T=\frac{\theta-\theta_0}{\theta_h-\theta_c},\quad \vec{B}=\frac{\vec{b}}{b_0},$$
$$Ra=\frac{g\beta(\theta_h-\theta_c)r_0^3}{\alpha v},\quad Pr=\frac{v}{\alpha},\quad \gamma=\frac{\chi_{m0}b_0^2}{\xi g r_0},$$

where τ is the dimensionless time, θ_0 is the reference temperature, θ_h is the hot plate temperature, θ_c is the cold plate temperature, α is the thermal diffusivity, v is the kinematic viscosity, γ is the ratio of the Kelvin force to the gravitational force, χ_{m0} is the mass magnetic susceptibility at the reference temperature and ξ is the magnetic permeability in a vacuum.

Here, reference values were defined as follows:

$$r_0=h,\quad u_0=\frac{\alpha}{r_0},\quad t_0=\frac{r_0}{u_0},$$
$$\theta_0=\frac{\theta_h+\theta_c}{2},\quad p_0=\rho_0 u_0^2,\quad b_0=\frac{\xi i}{r_0},$$

where h is the radius of a vertical cylindrical enclosure and i is the electric current in a circular electric coil.

3. Computational schemes

The dimensionless governing equations were numerically solved by a finite difference method. Inertial terms were approximated by the higher-order up-wind scheme called the UTOPIA scheme. Pressure and velocity corrections were solved with the HSMAC scheme (Hirt et al., 1975).

4. Model system

The simple model system shown in Fig. 1 was assumed in order to clarify the effect of the Kelvin force on the flow of water in a vertical cylindrical enclosure with a thermal gradient under a vertical magnetic field gradient. In this model system, the vertical cylindrical enclosure is assumed to be placed inside the bore space of a super-conducting magnet. The cylindrical enclosure is heated from below and cooled from above isothermally. The sidewall is thermally insulated. The broken line with the arrow shows a circular electric coil and the electric current circulating within the coil. The cylindrical enclosure and the circular electric coil are placed coaxially. The distribution of a vertical magnetic field was computed by Biot–Savart's law as shown in Eq. (14) for electric current circulating within a circular electric coil. The Kelvin force that is produced by the gradient of magnetic field is dependent on the position and the size of a circular electric coil. Therefore, the circular electric coil was placed either at the hot or the cold plate. In addition, the diameter of the circular electric coil was set to be 2.5 or 5 times that of the cylindrical enclosure.

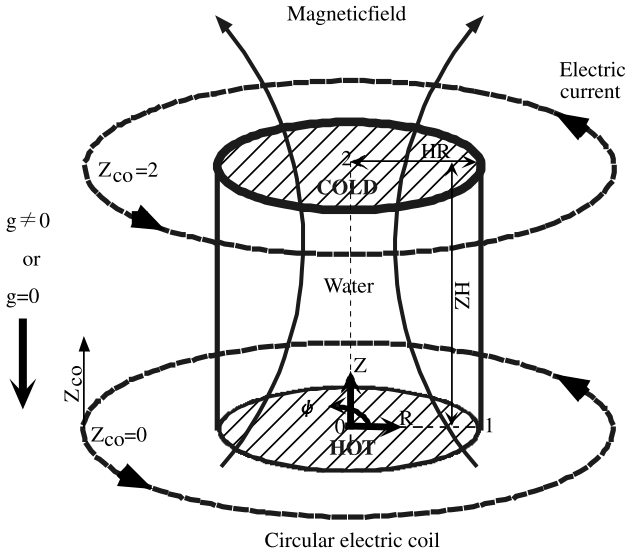

Fig. 1. Schematic representation of the model system used in the present numerical computations.

The numerical computations were carried out under the following conditions.

Initial conditions:

$$T=U=V=W=0\quad \text{at } \tau=0.$$

Boundary conditions:

$$T=+0.5,\ U=V=W=0\quad \text{at } 0\leqq R<\mathrm{HR} \text{ and } Z=0;$$
$$T=-0.5,\ U=V=W=0\quad \text{at } 0\leqq R<\mathrm{HR} \text{ and } Z=\mathrm{HZ};$$
$$\frac{\partial T}{\partial R}=0,\ U=V=W=0\quad \text{at } R=\mathrm{HR} \text{ and } 0<Z<\mathrm{HZ}.$$

5. Effect of computational grid number

In order to check the effect of computational grid number, sample computations were carried out for the

Table 1
Effect of grid number on average Nusselt number at the hot and cold plates ($Ra = 10^4$, $Pr = 5.85$)

$R\times Z$	The system without the magnetic field ($\gamma = 0$)			The system with the magnetic field ($\gamma = -400$ and $Z_{co} = 2$)		
	$(Nu_{ave})_c$	$(Nu_{ave})_h$	$(Nu_{ave})_c/(Nu_{ave})_h$	$(Nu_{ave})_c$	$(Nu_{ave})_h$	$(Nu_{ave})_c/(Nu_{ave})_h$
20×40	3.4828	3.3805	1.0303	7.7126	7.0709	1.0908
32×64	3.4364	3.4233	1.0038	7.7658	7.7286	1.0048
40×80	3.4283	3.4237	1.0013	7.7020	7.7067	0.99939

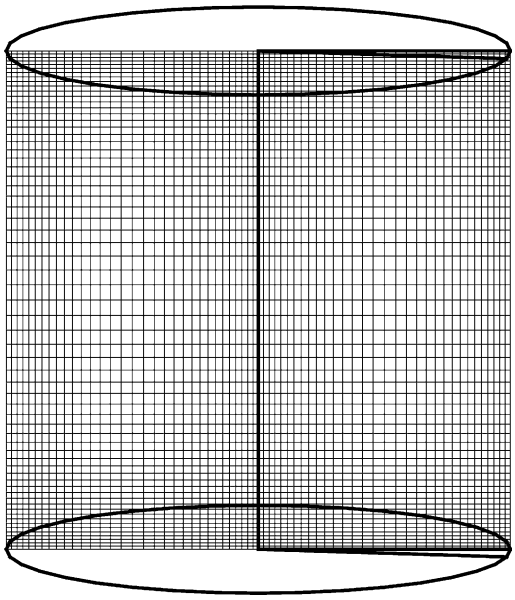

Fig. 2. Geometry of the enclosure and the grid of 32×64 in the radial and axial directions.

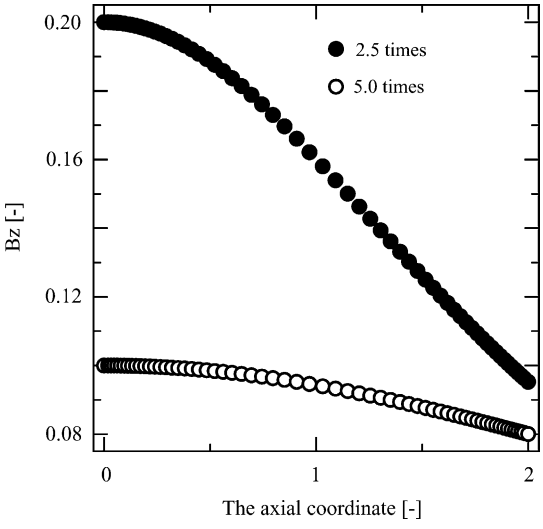

Fig. 3. An axial profile of the axial component of dimensionless magnetic induction (B_Z) on the centerline when the circular electric coil with 2.5 or 5 times the diameter of an enclosure was placed at the hot plate $Z_{co} = 0$.

Table 2
Physical properties of water at 0.1013 MPa and 300 K

Symbol	Property	Quantity	Unit
c_p	Specific heat capacity at constant pressure	4.177×10^3	J/(kg K)
β	Volumetric coefficient of expansion	2.7454×10^{-4}	K^{-1}
λ	Thermal conductivity	6.104×10^{-1}	W/(m K)
μ	Viscosity	8.544×10^{-4}	Pa s
ρ_0	Density	996.555	kg/m^3
χ_{m0}	Mass magnetic susceptibility	-9.0478×10^{-9}	m^3/kg

model system shown in Fig. 1. The domain within the vertical cylindrical enclosure was divided into small meshes with finer meshes near the wall and at the center of the enclosure. A staggered grid was employed so that the mass balance could be satisfied in each grid cell. Grid numbers of 20×40, 32×64, and 40×80 in the radial and axial directions were tested in the system with and without the magnetic field for $Ra = 10^4$, $Pr = 5.85$, and

Table 3
Reference values

Symbol	Property	Quantity	Unit
p_0	Reference pressure	2.143×10^{-7}	Pa
r_0	Radius of a vertical cylindrical enclosure	1.0×10^{-2}	m
t_0	Reference time	6.819×10^2	s
u_0	Reference velocity	1.466×10^{-5}	m/s
θ_0	Reference temperature	3.0×10^2	K

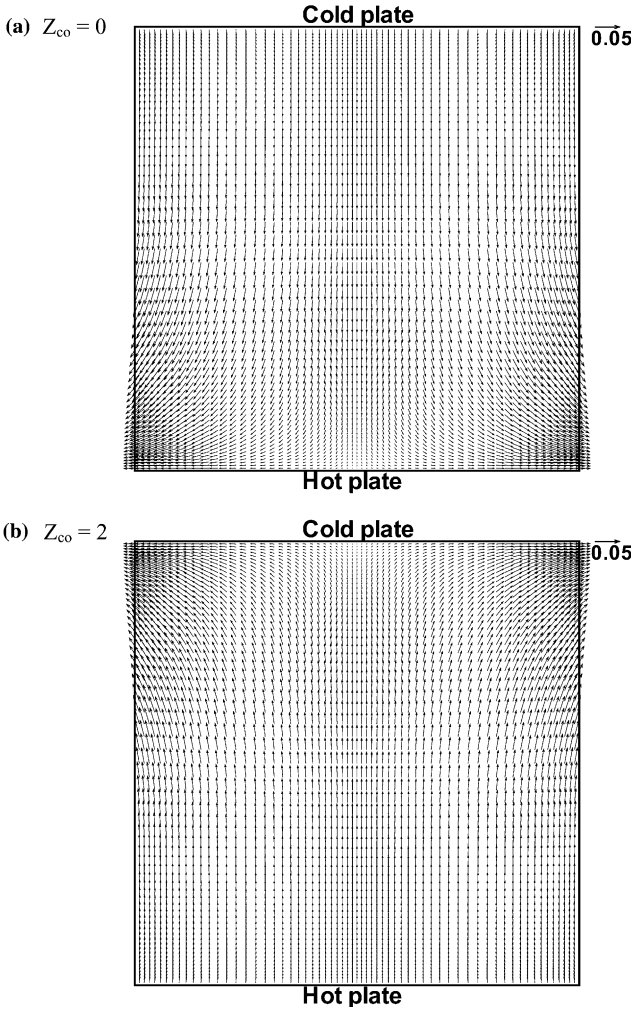

Fig. 4. The gradient of the square of magnetic induction (grad B^2) that is produced under a vertical magnetic field gradient when the circular electric coil with 2.5 times the diameter of the cylindrical enclosure was placed at (a) the hot plate $Z_{co} = 0$ and (b) the cold plate $Z_{co} = 2$.

$\gamma = 0$ or -400. The computed results of average Nusselt number at the hot and cold plates are listed in Table 1. In the system without the magnetic field $\gamma = 0$, the ratio of average Nusselt number at the hot and cold plates $(Nu_{ave})_c/(Nu_{ave})_h$ was 1.0303 for grids 20×40, 1.0038 for grids 32×64, and 1.0013 for grids 40×80. In the system with the magnetic strength of $\gamma = -400$ when the circular electric coil with 2.5 times the diameter of the vertical cylindrical enclosure was placed at the cold plate $Z_{co} = 2$, $(Nu_{ave})_c/(Nu_{ave})_h$ was 1.0908 for grids 20×40, 1.0048 for grids 32×64, and 0.99939 for grids 40×80. For grid numbers of 32×64 and 40×80, it is considered that the heat balance in the system with and without the magnetic field is almost maintained. Considering computational time, we used the grid of 32×64 in the subsequent computations, as seen in Fig. 2. This is because the main concern was to clarify the effect of Kelvin force on the flow of water rather than to determine accurate numerical values of the average Nusselt number.

6. Computed results

Fig. 3 shows an axial profile of the axial component of dimensionless magnetic induction (B_Z) on the centerline when the circular electric coil 2.5 or 5 times the diameter of the enclosure was placed at the hot plate $Z_{co} = 0$. Closed circles show the profile for the circular electric coil 2.5 times this diameter, and the open circles 5 times this diameter. Table 2 shows the physical properties of water (Gebhart et al., 1988; Japan Society of Thermophysical Properties, 2000; The Chemical Society of Japan, 2001) at 0.1013 MPa and 300 K. For a dia-

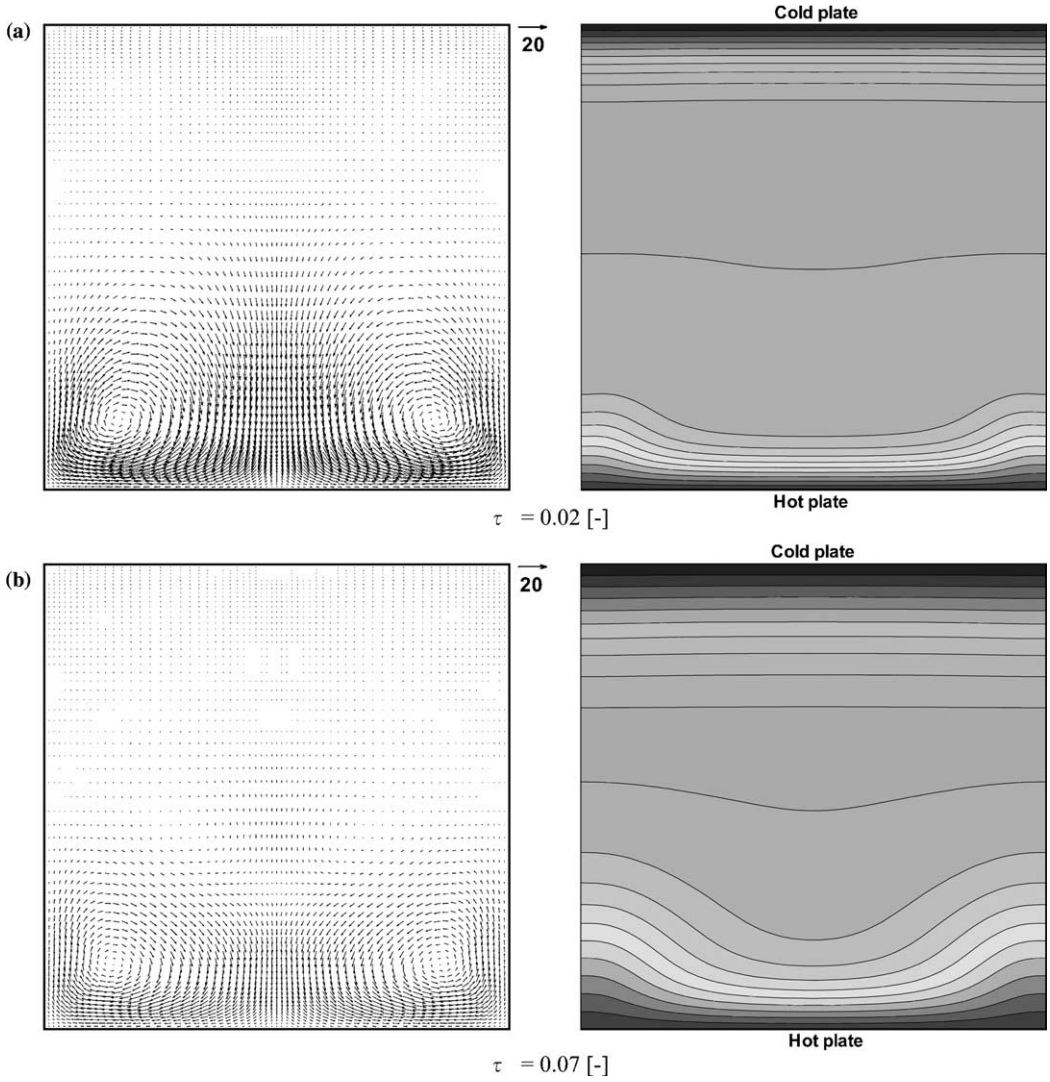

Fig. 5. The transition of velocity and temperature fields to the steady state when the circular electric coil with 2.5 times the diameter of the vertical cylindrical enclosure was placed at the hot plate under a non-gravitational field for $\gamma Ra = -2 \times 10^6$, $Pr = 5.85$, and $Z_{co} = 0$. (a) $\tau = 0.02$ [–] and (b) $\tau = 0.07$ [–].

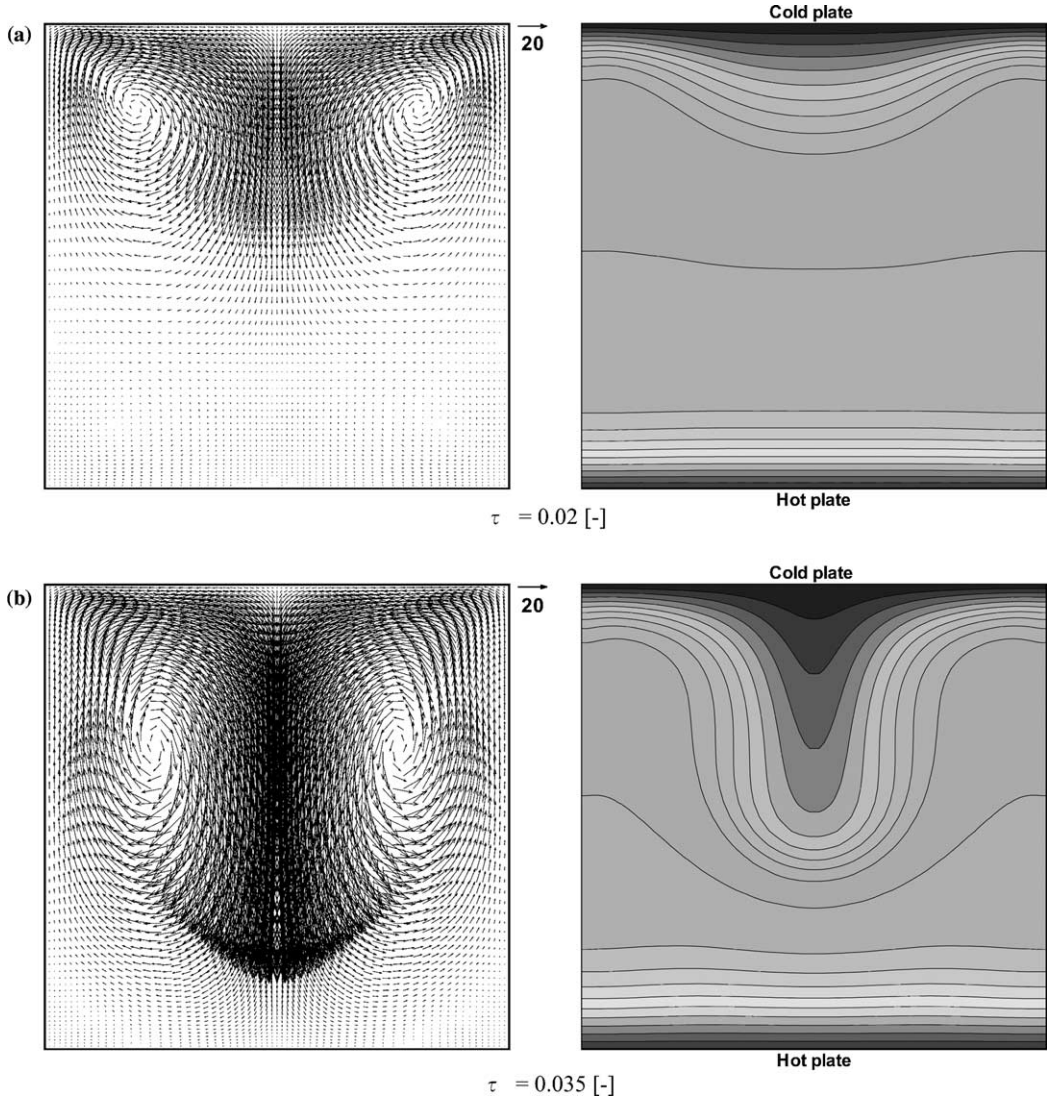

Fig. 6. The transition of velocity and temperature fields to the steady state when the circular electric coil with 2.5 times the diameter of the vertical cylindrical enclosure was placed at the cold plate under a non-gravitational field for $\gamma Ra = -2 \times 10^6$, $Pr = 5.85$, and $Z_{co} = 2$. (a) $\tau = 0.02$ and (b) $\tau = 0.035$.

magnetic substance such as water, the mass magnetic susceptibility has a negative value. Table 3 shows the reference values.

Fig. 4(a) and (b) shows the gradient of the square of magnetic induction (grad B^2) that is produced under a vertical magnetic field gradient when the circular electric coil with 2.5 times the diameter of the cylindrical enclosure was placed at (a) the hot plate $Z_{co} = 0$ and (b) the cold plate $Z_{co} = 2$.

Table 4
Average Nusselt number at the hot and cold plates in the steady state for the circular electric coil with 2.5 times the diameter of the vertical cylindrical enclosure in a non-gravitational field ($Pr = 5.85$)

γRa	$Z_{co} = 0$		$Z_{co} = 2$	
	$(Nu_{ave})_c$	$(Nu_{ave})_h$	$(Nu_{ave})_c$	$(Nu_{ave})_h$
-2×10^6	1.0598	1.0611	5.7205	5.7243

To begin, we carried out the numerical computations in a non-gravitational field to clarify the effect of Kelvin force alone. In a gravitational field, the governing parameters are the Prandtl number (Pr), the Rayleigh number (Ra), and the ratio of the Kelvin force to the gravitational force (γ). However, in a non-gravitational field, Ra becomes zero and γ becomes infinity. To circumvent these problems, the product of γ by Ra was used as one of the governing parameters in a non-gravitational field. This is because the gravity is eliminated. As a result, in a non-gravitational field, the right side in Eq. (12) consists of the terms of pressure, viscosity, and Kelvin force so that the buoyancy term is eliminated.

Table 5
Maximum axial velocity at the central axis W_{max} and average Nusselt number at the hot plate $(Nu_{ave})_h$ for the circular electric coil with 2.5 or 5 times the diameter of the vertical cylindrical enclosure in a gravitational field ($Ra = 10^4$, $Pr = 5.85$)

γ	2.5 times				5 times			
	$Z_{co} = 0$		$Z_{co} = 2$		$Z_{co} = 0$		$Z_{co} = 2$	
	W_{max}	$(Nu_{ave})_h$	W_{max}	$(Nu_{ave})_h$	W_{max}	$(Nu_{ave})_h$	W_{max}	$(Nu_{ave})_h$
0	−87.53	3.4233	−87.53	3.4233	−87.53	3.4233	−87.53	3.4233
−50	−51.51	3.0468	−130.9	4.6578	−85.16	3.4611	−92.17	3.5609
−100	−15.58	1.3341	−165.3	5.3750	−82.41	3.4737	−96.59	3.6847
−200	−8.818	1.1350	−224.0	6.3852	−76.22	3.4532	−104.9	3.9049
−300	−8.064	1.1205	−274.7	7.1301	−69.57	3.3856	−112.9	4.1008
−400	−8.026	1.1163	−320.1	7.7286	−62.62	3.2663	−120.5	4.2771

Figs. 5 and 6 show the computed results in a non-gravitational field. Fig. 5 shows the transition of velocity and temperature fields to the steady state when the circular electric coil with 2.5 times the diameter of the vertical cylindrical enclosure was placed at the hot plate for $\gamma Ra = -2 \times 10^6$, $Pr = 5.85$, and $Z_{co} = 0$. For this case, the gradient of the square of magnetic induction is produced as shown in Fig. 4(a). Under the initial conditions of $T = U = V = W = 0$, by applying thermal and magnetic field gradients, the magnetothermal convection slightly developed only near the hot plate, as seen in Fig. 5(a). Subsequently, the magnetothermal convection hardly developed, as seen in Fig. 5(b). Corresponding figures for $\gamma Ra = -2 \times 10^6$, $Pr = 5.85$, and $Z_{co} = 2$ are shown in Fig. 6. For this case, the gradient of the square of magnetic induction is produced as shown in Fig. 4(b). In the first place, the magnetothermal convection was induced only near the cold plate, as seen in Fig. 6(a). Subsequently, the magnetothermal convection gradually developed with time, as seen in Fig. 6(b). Finally, the low-temperature fluid near the central axis collided with the hot plate. From Figs. 5 and 6, it is shown that the magnetothermal convection was induced from the vicinity of the circular electric coil. The average Nusselt number at the hot and cold plates in the steady state for these cases is listed in Table 4. We also carried out the numerical computations for $\gamma Ra = -2 \times 10^6$, $Pr = 5.85$, and $Z_{co} = 0$ or 2 under the initial conditions of $T = 0.5(1 - Z)$ and $U = V = W = 0$. For these cases, the transition of velocity and temperature fields to the steady state was almost the same as those in Figs. 5 and 6, and transient computations converged earlier than those under the initial conditions of $T = U = V = W = 0$. The Kelvin force term depends on γRa, Pr, T and the gradient of the square of magnetic induction. However, it was shown that the solution at the steady state was not dependent on the temperature field of the initial condition.

In order to estimate the contribution of gravitational buoyant force, we then carried out the numerical computations including a gravitational field. Transient computation converged under all numerical conditions. The numerical data of the maximum axial velocity at the central axis W_{max} and the average Nusselt number at the hot plate $(Nu_{ave})_h$ for the circular electric coil with 2.5 or 5 times the diameter of the vertical cylindrical enclosure in a gravitational field are listed in Table 5. The axial velocity with the negative value shows the flow of the gravity direction. The average Nusselt number at the hot plate in a gravitational field is summarized in Fig. 7. A cross symbol indicates the value in the system without the magnetic field. In Fig. 8, velocity vectors, temperature contours, and isothermal planes at the steady state in the system without the magnetic field are shown. In the system with the magnetic field, the average Nusselt number strongly depended on the size and the axial position of a circular electric coil in addition to the magnetic strength, as shown in Fig. 7. By placing the circular electric coil at the hot plate $Z_{co} = 0$, the average Nusselt number decreased with the increase of $|\gamma|$. Under the circular electric coil with 2.5 times the diameter of the enclosure, the conduction state was nearly attained for $\gamma = -200$ and $Z_{co} = 0$. In Fig. 9,

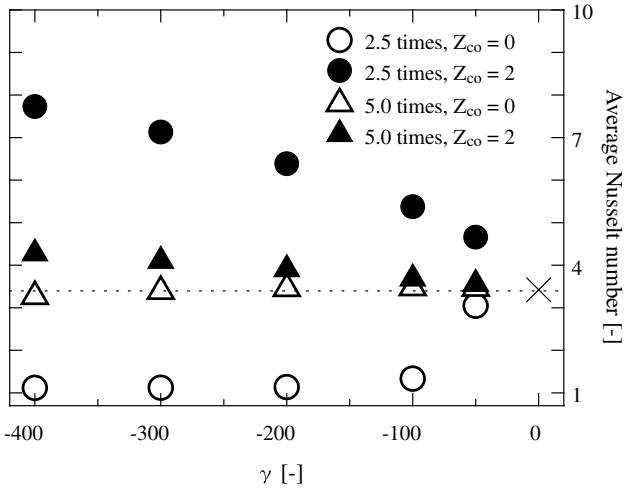

Fig. 7. Average Nusselt number at the hot plate $(Nu_{ave})_h$ versus the strength of the magnetic field γ in a gravitational field for the circular electric coil with 2.5 or 5 times the diameter of the vertical cylindrical enclosure at $Ra = 10^4$ and $Pr = 5.85$. A cross symbol indicates $(Nu_{ave})_h$ without a magnetic field.

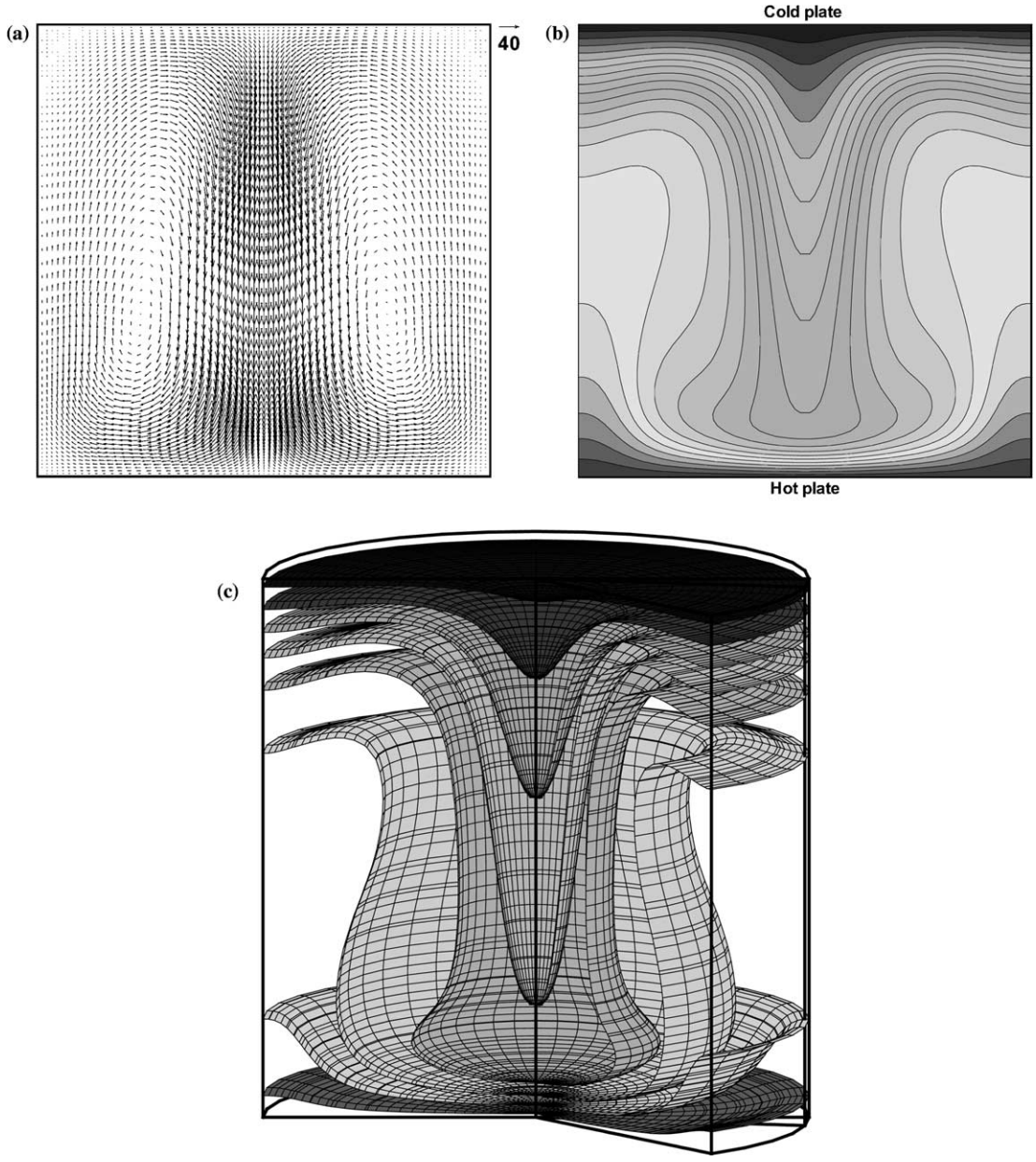

Fig. 8. (a) Velocity vectors, (b) temperature contours, and (c) isothermal planes at the steady state in the system without the magnetic field for $Ra = 10^4$, $Pr = 5.85$, and $\gamma = 0$.

velocity vectors, temperature contours, and isothermal planes at the steady state for this case are shown. The transition of velocity and temperature fields to the steady state was almost the same as that in a non-gravitational field, as shown in Fig. 5. This result indicates that the Kelvin force overcomes buoyant gravitational force. In a vertical cylindrical enclosure with a magnetic field gradient, as shown in Fig. 4(a), the high-temperature fluid near the hot plate receives both the radial Kelvin force towards the sidewall from the centerline and the axial Kelvin force toward the hot plate; the low-temperature fluid near the cold plate receives the axial Kelvin force towards the cold plate, as shown in Fig. 11(a). Namely, it is considered that the natural convection cannot develop by these Kelvin forces. On the other hand, by placing the circular electric coil at the cold plate $Z_{co} = 2$, the reverse tendency was computed; i.e., the average Nusselt number increased with the increase of $|\gamma|$, as seen in Fig. 7. Under the circular electric coil with 2.5 times the diameter of an enclosure for $\gamma = -400$ and $Z_{co} = 2$, the average Nusselt number became about 2.3 times that for $\gamma = 0$. In Fig. 10, velocity vectors, temperature contours, and isothermal planes at the steady state for $\gamma = -200$ and $Z_{co} = 2$ are shown. In a vertical cylindrical enclosure with a magnetic field gradient, as shown in Fig. 4(b), the high-temperature fluid near the hot

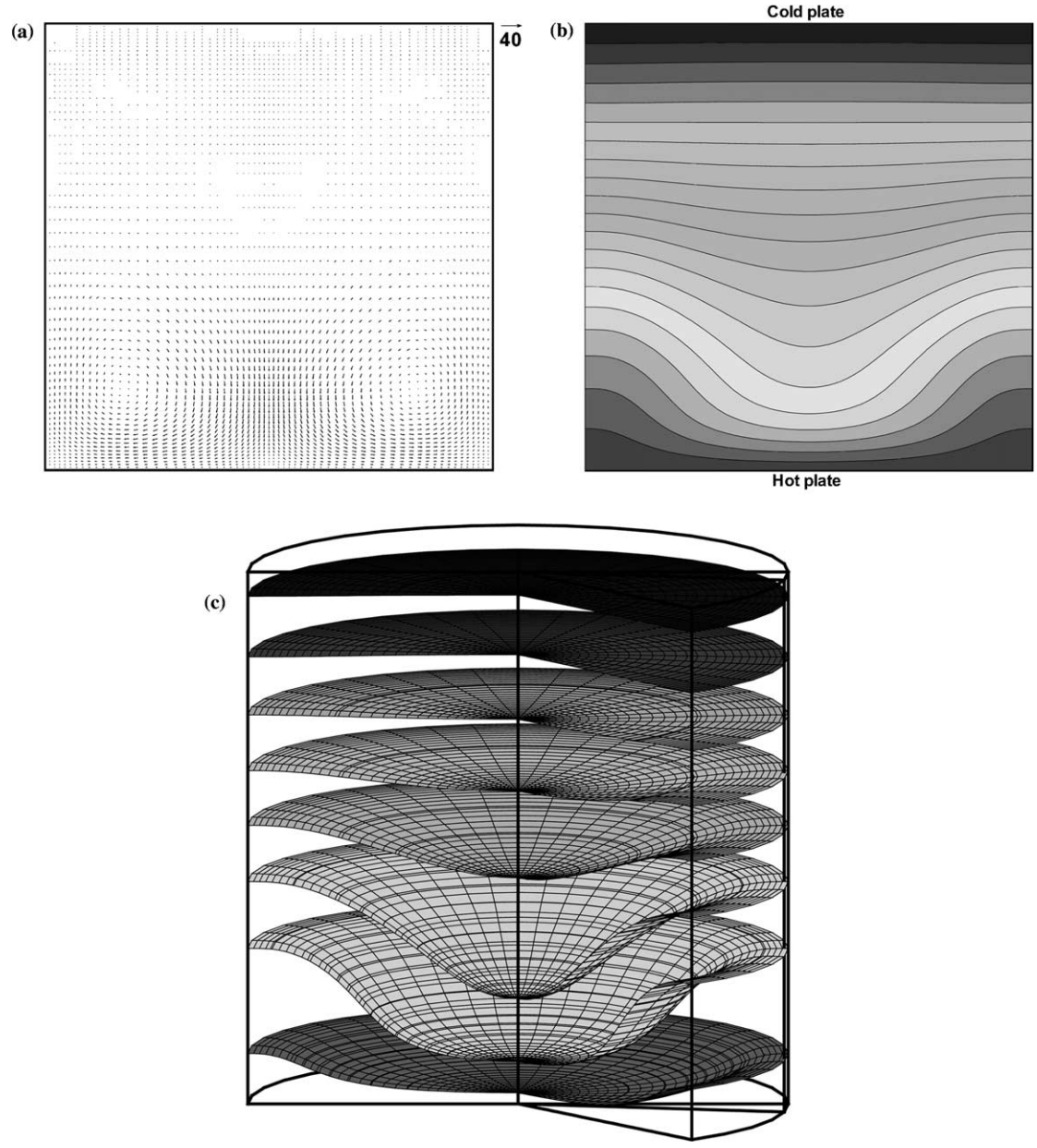

Fig. 9. (a) Velocity vectors, (b) temperature contours, and (c) isothermal planes at the steady state in the system with the magnetic field when the circular electric coil with 2.5 times the diameter of the vertical cylindrical enclosure was placed at $Z_{co} = 0$ for $Ra = 10^4$, $Pr = 5.85$, and $\gamma = -200$.

plate receives the axial Kelvin force toward the cold plate; the low-temperature fluid near the cold plate receives both the radial Kelvin force toward the centerline from the sidewall and the axial Kelvin force toward the hot plate, as shown in Fig. 11(b). Namely, it is considered that the natural convection is enhanced by these Kelvin forces.

Here, when the radius of a cylindrical enclosure is $r_0 = 1.0 \times 10^{-2}$ m, dimensional velocity -320 corresponds to -4.69×10^{-3} m/s. The maximum temperature difference $\theta_h - \theta_c$ is 0.47 K at $Ra = 10^4$. When the strength of a magnetic field is $\gamma = -400$, the maximum value of b_Z at the central axis is about 14.8 T for the circular electric coil with 2.5 times the diameter of an enclosure and about 7.38 T for the circular electric coil with 5 times the diameter of an enclosure.

7. Conclusions

The present study focused on how a Kelvin force affects the flow of water with the diamagnetic property in an enclosure with thermal and magnetic gradients. Two-dimensional numerical computations were carried out

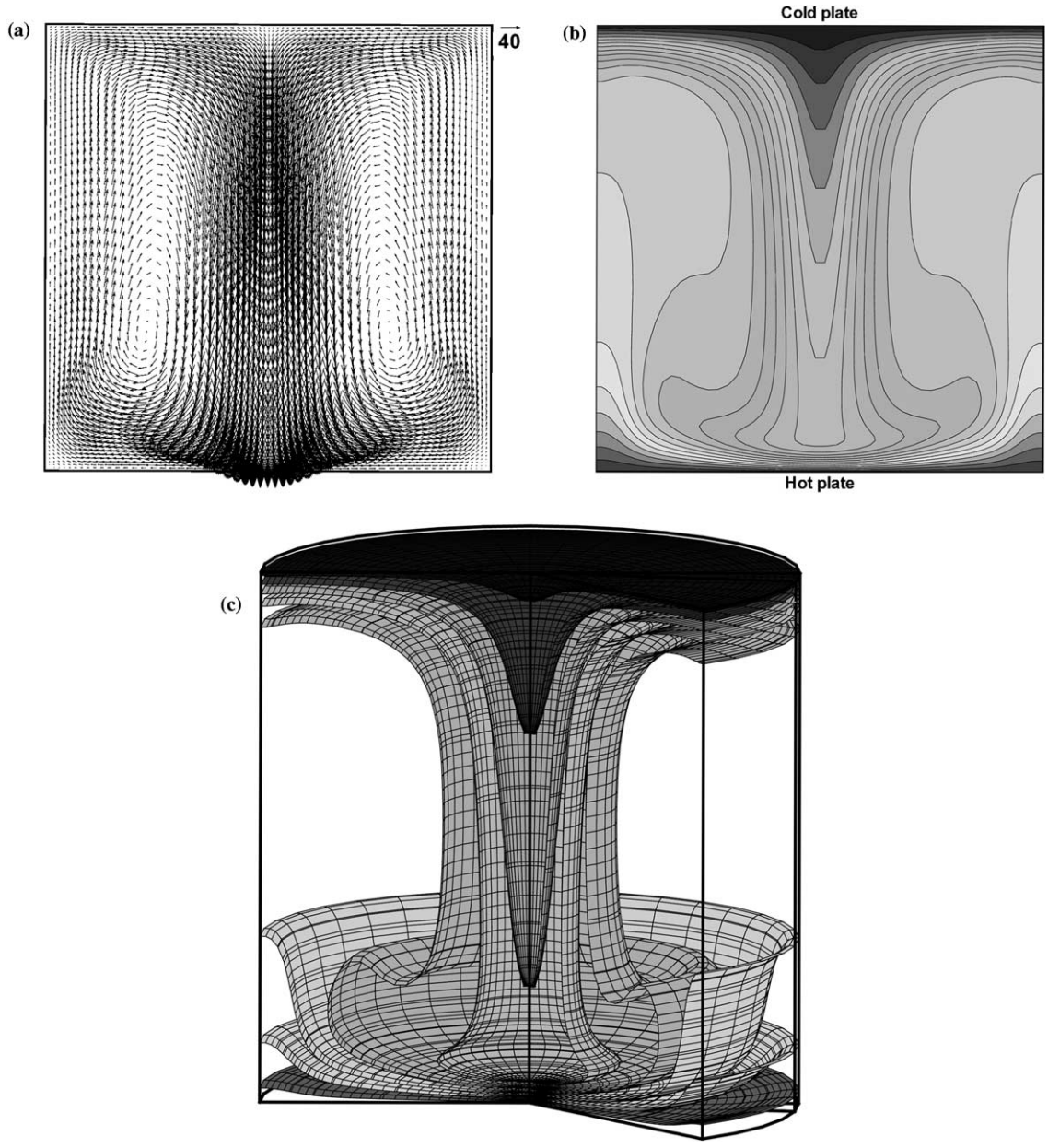

Fig. 10. (a) Velocity vectors, (b) temperature contours, and (c) isothermal planes at the steady state in the system with the magnetic field when the circular electric coil with 2.5 times the diameter of the vertical cylindrical enclosure was placed at $Z_{co} = 2$ for $Ra = 10^4$, $Pr = 5.85$, and $\gamma = -200$.

using the model system of the vertical cylindrical enclosure heated from below and cooled from above under a vertical magnetic field gradient, and we concluded the following.

When the circular electric coil is placed at the lower end plate which is heated isothermally, the Kelvin force suppresses the generation of natural convection of water. When the circular electric coil is placed at the upper end plate, which is cooled isothermally, the Kelvin force enhances the natural convection of water. The Kelvin force varies with the density and the gradient of the square of magnetic induction. In the enclosure with thermal and magnetic gradients, the Kelvin force acts on the high-temperature water with a small density as the attractive force and the low-temperature water with a large density as the repulsive force. When the circular electric coil is placed at the cold plate, the colder fluid is repelled from the higher magnetic field region and the hotter fluid is attracted toward the higher magnetic field region. Therefore, the natural convection is enhanced by the Kelvin force. Even in a non-gravitational field, the Kelvin force destabilizes the water in the quiescent conduction state.

Our numerical results suggest that the Kelvin force can be utilized to control the flow and the heat transfer rate of diamagnetic fluid in an enclosure with thermal

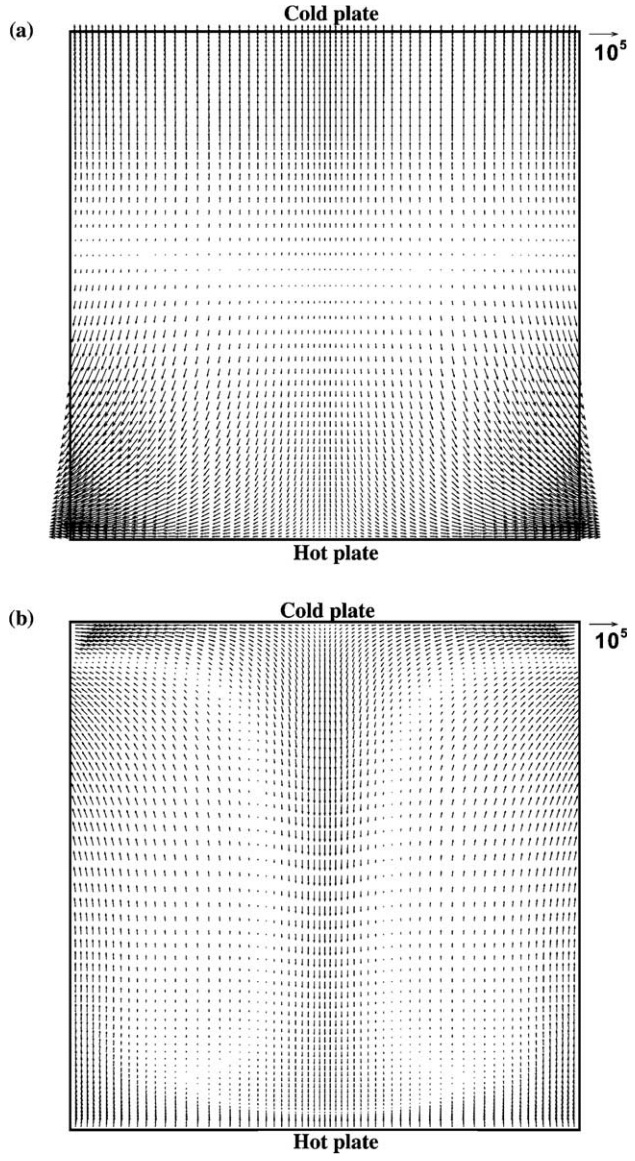

Fig. 11. The Kelvin force ($-0.5\gamma RaPrT\,\mathrm{grad}\,B^2$) that is produced under a vertical magnetic field gradient when the circular electric coil with 2.5 times the diameter of the vertical cylindrical enclosure was placed at (a) the hot plate $Z_{co} = 0$ and (b) the cold plate $Z_{co} = 2$ for $Ra = 10^4$, $Pr = 5.85$, and $\gamma = -200$.

and magnetic gradients under both gravitational and non-gravitational fields. However, there is yet no experimental data on the model system using the present computation. Therefore, experimental results will need to be obtained to prove these numerical results.

Acknowledgments

The authors wish to acknowledge financial support from the Sumitomo Foundation (grant no. 030510) for this work.

References

Akamatsu, M., Higano, M., Takahashi, Y., Ozoe, H., 2003. Numerical computation on the control of aerial flow by the magnetizing force in gravitational and non-gravitational fields. Num. Heat Transfer Part A 43 (1), 9–29.

Akamatsu, M., Higano, M., Takahashi, Y., Ozoe, H., 2005. Heat transfer control in quiescent air with thermal gradient by magnetizing force under both gravitational and non-gravitational fields. Num. Heat Transfer Part A 47 (4), 375–392.

Bai, B., Yabe, A., Qi, J., Wakayama, N.I., 1999. Quantitative analysis of air convection caused by magnetic–fluid coupling. AIAA J. 37 (12), 1538–1543.

Berry, M.V., Geim, A.K., 1997. Of flying frogs and levitrons. Eur. J. Phys. 18 (4), 307–313.

Braithwaite, D., Beaugnon, E., Tournier, R., 1991. Magnetically controlled convection in a paramagnetic fluid. Nature 354 (14), 134–136.

Carruthers, J.R., Wolfe, R., 1968. Magnetothermal convection in insulating paramagnetic fluids. J. Appl. Phys. 39 (12), 5718–5722.

Chandrasekhar, S., 1981. Hydrodynamics and Hydromagnetic Stability. Dover Publ. Inc., New York.

Cini, R., Torrini, M., 1968. Temperature dependence of the magnetic susceptibility of water. J. Chem. Phys. 49 (6), 2826–2830.

Faraday, M., 1847. On the diamagnetic conditions of flame and gases. Phil. Mag. S.3 31 (210), 401–421.

Gebhart, B., Jaluria, Y., Mahajan, R.L., Sammakia, B., 1988. Buoyancy-Induced Flows and Transport. Hemisphere Pub., New York, pp. 946–947.

Gray, D.D., Huang, J., Edwards, B.F., 2001. Two-dimensional magnetothermal plumes. Int. J. Eng. Sci. 39 (16), 1837–1861.

Hirt, C.W., Nichols, B.D., Romero, N.C., 1975. A numerical solution algorithm for transient fluid flows. Tech. Rept., Los Alamos Sci. Lab., LA-5852.

Japan Society of Thermophysical Properties, 2000. Thermophysical Properties Handbook. YOKENDO Ltd., Tokyo, p. 64 (in Japanese).

Kaneda, M., Tagawa, T., Ozoe, H., 2002a. Convection induced by a cusp-shaped magnetic field for air in a cube heated from above and cooled from below. J. Heat Transfer 124 (1), 17–25.

Kaneda, M., Tagawa, T., Ozoe, H., 2002b. Numerical analyses for magnetically enhanced natural convection of air in an inclined rectangular enclosure heated from below. J. Enhanced Heat Transfer 9 (2), 89–97.

Kaneda, M., Tagawa, T., Ozoe, H., 2002c. Effect of the Rayleigh number on the magnetizing force convection in a cube with cusp-shaped magnetic field. Prog. Comput. Fluid Dyn. 2 (2–4), 72–79.

Maki, S., Tagawa, T., Ozoe, H., 2002. Enhanced convection or quasi-conduction states measured in a super-conducting magnet for air in a vertical cylindrical enclosure heated from below and cooled from above in a gravity field. J. Heat Transfer 124 (4), 667–673.

Pauling, L., Wood, R.E., Sturdivant, J.H., 1946. An instrument for determining the partial pressure of oxygen in a gas. J. Am. Chem. Soc. 68, 795–798.

Qi, J., Wakayama, N.I., Yabe, A., 1999. Attenuation of natural convection by magnetic force in electro-nonconducting fluids. J. Cryst. Growth 204 (3), 408–412.

Qi, J., Wakayama, N.I., Yabe, A., 2001a. Magnetic control of thermal convection in electrically non-conducting or low-conducting paramagnetic fluids. Int. J. Heat Mass Transfer 44 (16), 3043–3052.

Qi, J., Wakayama, N.I., Ataka, M., 2001b. Magnetic suppression of convection in protein crystal growth processes. J. Cryst. Growth 232 (1), 132–137.

Rosensweig, R.E., 1985. Ferrohydrodynamics. Cambridge Univ. Press, London.

Shigemitsu, R., Tagawa, T., Ozoe, H., 2003. Numerical computation for natural convection of air in a cubic enclosure under combination of magnetizing and gravitational forces. Num. Heat Transfer Part A 43 (5), 449–463.

Tagami, M., Hamai, M., Mogi, I., Watanabe, K., Motokawa, M., 1999. Solidification of levitating water in a gradient strong magnetic field. J. Cryst. Growth 203 (4), 594–598.

Tagawa, T., Ozoe, H., Inoue, K., Ito, M., Sassa, K., Asai, S., 2001. Transient characteristics of convection and diffusion of oxygen gas in an open vertical cylinder under magnetizing and gravitational forces. Chem. Eng. Sci. 56 (14), 4217–4223.

Tagawa, T., Ozoe, H., Sassa, K., Asai, S., 2002a. Convective and diffusive phenomena of air in a vertical cylinder under a strong magnetic field. Num. Heat Transfer Part B 41 (3–4), 383–395.

Tagawa, T., Shigemitsu, R., Ozoe, H., 2002b. Magnetizing force modeled and numerically solved for natural convection of air in a cubic enclosure: effect of the direction of the magnetic field. Int. J. Heat Mass Transfer 45 (2), 267–277.

Tagawa, T., Ujihara, A., Ozoe, H., 2003. Numerical computation for Rayleigh–Benard convection of water in a magnetic field. Int. J. Heat Mass Transfer 46 (21), 4097–4104.

The Chemical Society of Japan, 2001. Handbook of Chemistry, Basic 4th ed. MARUZEN, Tokyo, p. II-508 (in Japanese).

Uetake, H., Nakagawa, J., Hirota, N., Kitazawa, K., 1999. Nonmechanical magnetothermal wind blower by a superconducting magnet. J. Appl. Phys. 85 (8), 5735–5737.

Wakayama, N.I., 1991a. Effect of a decreasing magnetic field on the flow of nitrogen gas. Chem. Phys. Lett. 185 (5–6), 449–451.

Wakayama, N.I., 1991b. Behavior of gas flow under gradient magnetic fields. J. Appl. Phys. 69 (4), 2734–2736.

Wakayama, N.I., Ataka, M., Abe, H., 1997. Effect of a magnetic field gradient on the crystallization of hen lysozyme. J. Cryst. Growth 178 (4), 653–656.